

## A high-temperature calorimetric flow sensor employing ion conduction in zirconia

A. Persson, V. Lekholm, G. Thornell, and L. Klintberg

Citation: [Applied Physics Letters](#) **106**, 194103 (2015); doi: 10.1063/1.4921051

View online: <http://dx.doi.org/10.1063/1.4921051>

View Table of Contents: <http://scitation.aip.org/content/aip/journal/apl/106/19?ver=pdfcov>

Published by the [AIP Publishing](#)

---

### Articles you may be interested in

[Ion conduction in nanoscale yttria-stabilized zirconia fabricated by atomic layer deposition with various doping rates](#)

*J. Vac. Sci. Technol. A* **31**, 01A107 (2013); 10.1116/1.4755921

[Interface proximity effects on ionic conductivity in nanoscale oxide-ion conducting yttria stabilized zirconia: An atomistic simulation study](#)

*J. Chem. Phys.* **134**, 064703 (2011); 10.1063/1.3549891

[High temperature conductivity studies on nanoscale yttria-doped zirconia thin films and size effects](#)

*Appl. Phys. Lett.* **89**, 183116 (2006); 10.1063/1.2385211

[High-temperature stability of ion-implanted zirconia and spinel](#)

*J. Appl. Phys.* **97**, 113509 (2005); 10.1063/1.1924879

[Fundamental functions of a new type of leak detector using oxygen-ion conductor](#)

*J. Vac. Sci. Technol. A* **18**, 1755 (2000); 10.1116/1.582419

---

An advertisement for COMSOL simulation software. On the left, a dark blue box contains the text 'CREATE your best design' in white and yellow. In the center, a white box lists various simulation parameters for a TE11 cutoff frequency, such as Frequency (4.868 Hz), Wavelength (0.5205 m), Flare angle (17 degrees), and others. On the right, a 3D simulation model of a horn antenna is shown with a color-coded field distribution. At the bottom, the text 'WITH SIMULATION APPS >>' and the COMSOL logo are displayed.

TE11 cutoff frequency (fc):	4.868 Hz
Frequency:	fc*1.2 Hz
Wavelength (lambda):	0.5205 m
Flare angle:	17 °
Corrugation thickness:	0.105 m
Corrugation length:	0.155 m
Horn thickness:	0.5 m
Horn length:	4 m
Waveguide length:	1 m
Matching corrugation length:	0.25 m

Input waveguide cross pol. ratio: 17.657 %  
Output aperture cross pol. ratio: 3.025 %  
 Target criterion: passed

## A high-temperature calorimetric flow sensor employing ion conduction in zirconia

A. Persson,<sup>1,2,a)</sup> V. Lekholm,<sup>1,2</sup> G. Thornell,<sup>1,2</sup> and L. Klintberg<sup>2</sup>

<sup>1</sup>Department of Engineering Sciences, Ångström Space Technology Center, Uppsala University, Box 534, 751 21 Uppsala, Sweden

<sup>2</sup>Department of Engineering Sciences, Uppsala University, Box 534, 751 21 Uppsala, Sweden

(Received 30 January 2015; accepted 1 May 2015; published online 12 May 2015)

This paper presents the use of the temperature-dependent ion conductivity of 8 mol % yttria-stabilized zirconia (YSZ8) in a miniature high-temperature calorimetric flow sensor. The sensor consists of 4 layers of high-temperature co-fired ceramic (HTCC) YSZ8 tape with a 400  $\mu\text{m}$  wide, 100  $\mu\text{m}$  deep, and 12 500  $\mu\text{m}$  long internal flow channel. Across the center of the channel, four platinum conductors, each 80  $\mu\text{m}$  wide with a spacing of 160  $\mu\text{m}$ , were printed. The two center conductors were used as heaters, and the outer, up- and downstream conductors were used to probe the resistance through the zirconia substrate around the heaters. The thermal profile surrounding the two heaters could be made symmetrical by powering them independently, and hence, the temperature sensing elements could be balanced at zero flow. With nitrogen flowing through the channel, forced convection shifted the thermal profile downstream, and the resistance of the temperature sensing elements diverged. The sensor was characterized at nitrogen flows from 0 to 40 sccm, and resistances at zero-flow from 10 to 50 M $\Omega$ . A peak sensitivity of 3.1 M $\Omega$ /sccm was obtained. Moreover, the sensor response was found to be linear over the whole flow range, with  $R^2$  of around 0.999, and easy to tune with the individual temperature control of the heaters. The ability of the sensor to operate in high temperatures makes it promising for use in different harsh environments, e.g., for close integration with microthrusters. © 2015 AIP Publishing LLC.

[<http://dx.doi.org/10.1063/1.4921051>]

In microsystems technology, zirconia ( $\text{ZrO}_2$ ) has been used as a substrate material in high-temperature applications, because of its excellent thermomechanical properties.<sup>1–3</sup> One such application is miniaturized low-thrust propulsion for small spacecraft, where the impulse of the thruster can be increased by electrically heating the gas in a stagnation chamber before expelling it.<sup>4,5</sup> To control the impulse, it is useful to integrate a sensor that monitors the gas flow through the nozzle. However, although the thermal conductivity of zirconia is relatively low, even in comparison with other engineering ceramics,<sup>6</sup> a calorimetric flow sensor integrated in the nozzle has been shown to be affected by thermal cross-talk from the heater.<sup>1</sup>

Doping zirconia with yttrium oxide ( $\text{Y}_2\text{O}_3$ ), creates high ion conductivity at high temperatures,<sup>7–9</sup> which is utilized, e.g., in solid-oxide fuel cells.<sup>10,11</sup> Above 700 °C, or at low oxygen partial pressure, the ionic part of the conductivity is dominated by movement of oxygen point defects.<sup>7</sup> Zirconia is frequently used for miniaturized gas sensors,<sup>12–14</sup> since its surface conductivity also depends on the partial pressure of oxygen.<sup>9</sup> The above-mentioned calorimetric flow sensor<sup>1,15</sup> requires electrical isolation, otherwise the conductivity of the substrate will disturb the signal by electrical cross-talk;<sup>15</sup> wherefore, only temperatures where the ion conductivity is negligible can be permitted, limiting the thruster's performance and the level of integration.

Typically, calorimetric flow sensors consist of a heater element between an upstream and a downstream resistive temperature sensor element,<sup>16,17</sup> or similar. A flow will make the temperature profile of the heated gas asymmetric, and accordingly, the two sensor elements will report different temperatures. Miniature sensors of this kind have been realized in silicon,<sup>16,18,19</sup> low-temperature co-fired ceramics,<sup>20</sup> and polymers,<sup>17</sup> and are also commercially available with a linear temperature response over several hundred Kelvin.

In this exploratory study, we exploit the strong, exponential temperature dependence of zirconia's ion conductivity in a calorimetric flow sensor, and investigate if the previously reported disadvantage can make the sensor more sensitive.

The sensor used here closely resembles those in previous work,<sup>15</sup> but contains four 80  $\mu\text{m}$  wide platinum conductors with a separation of 160  $\mu\text{m}$ , across a 400  $\mu\text{m}$  wide, 100  $\mu\text{m}$  deep, and 12 500  $\mu\text{m}$  long fluidic channel, Figure 1, inside a 400  $\mu\text{m}$  thick stack of four laminated high-temperature co-fired ceramic (HTCC) tapes.

Green tapes of 8 mol. % yttria stabilized zirconia (YSZ8, ESL 42401, Electroscience Laboratories, USA), having a thickness of 125  $\mu\text{m}$ , were punched using silicon tools fabricated by deep reactive ion etching (DRIE) to a depth of 75  $\mu\text{m}$ . A printed circuit board (PCB) press (RMP 210, Bungard, Belgium) was used to emboss the contour of the channel, along with two gas vias in the top two layers of the stack, at room temperature, and a pressure of 8 MPa. After removing the material within the embossed contours, the

<sup>a)</sup>Electronic mail: anders.persson@angstrom.uu.se

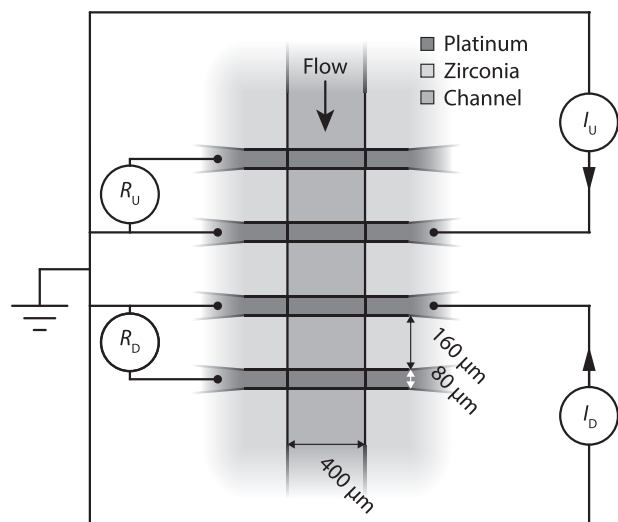


FIG. 1. Flow channel of the sensor with the middle two, separately powered, conductors used as heaters, and the zirconia resistance measured upstream and downstream of the heaters.

flow channel was filled with sacrificial material (ESL 49000, Electroscience Laboratories, USA). Platinum (ESL 5542, Electroscience Laboratories, USA) was screen printed on the third tape, pre-laminated to the fourth, to form conductive elements at the bottom of the channel, after which all layers were stacked and laminated in the press at 70 °C and 21 MPa for 15 min. The stack was sintered in air at 1450 °C for 90 min after the organic filler and binder in the tape had been burned off.<sup>1,15</sup>

In order to achieve robust connections, the component was glued (Epoxy Rapid, Bostik, Australia) to a custom made PCB with pin headers. Each platinum lead was connected to the PCB with four  $\varnothing$  25  $\mu$ m gold wires. A  $\varnothing$  6 mm tube (PA12 PL 6  $\times$  1, Bosch Rexroth, Germany) was glued to the inlet of the channel and connected to the front end of a flow setup,<sup>15</sup> where pure nitrogen gas was fed to the sensor through a toggle valve (SS-1GS4, Swagelok, USA), two filters (SS-4F-90 and SS-4TF-7, Swagelok, USA), a servo valve (Series 216, Granville-Phillips, USA), a pressure sensor (Standard industrial 0–1 MPa, Swagelok, USA), and finally, through a mass flow sensor (0–1000 sccm, Honeywell International Inc., USA).

The two center conductors of the sensor were used as heaters, and were connected to separate current sources (Dual port QL355TP, Thurlby Thandar Instruments, UK), Figure 1. The resistance in the zirconia adjacent to the heaters was measured by connecting two desktop multimeters—a HP 34410 (Hewlett Packard, USA) and a Keithley 2010 (Keithley Instruments Inc., USA)—between the two outer conductors and the common ground, Figure 1. The bias currents of the multimeters were in the sub-microampere range. With this scheme, the resistance in the zirconia upstream and downstream of the heaters could be measured while varying the flow through the channel and the power supplied to the heaters. The individually controlled heaters were allowed for balancing of the temperature profile, so that the upstream and downstream resistances were equal at zero flow for all temperatures.

The resistance at zero flow was obtained by adjusting the current through the heaters and stabilizing their temperature for about 10 min, before equalizing the upstream and downstream resistances by fine-tuning the heater currents. Then, to characterize the sensor, the flow was rapidly (in about 10 s) increased to about 40 sccm, after which the toggle valve was closed, and the sensor response was monitored while the flow slowly (in about 180 s) fell back to zero. During this, the resistances were sampled at 1.5 Hz, whereas the flow was sampled at  $\sim$ 15 Hz. The resistance time series were later interpolated to account for the higher sampling frequency of the flow measurements. After reaching zero flow, the procedure was repeated to cover a resistances at zero flow of 10, 20, 30, 40, and 50 M $\Omega$ , where the experiment at 20 M $\Omega$  was repeated three times to study the reproducibility of the results.

In a second experiment, the resistance between two adjacent elements was recorded while varying the ambient temperature from 400 °C to 650 °C in a furnace (Thermolyne FB1310M, Thermo Scientific, USA). Here, the sample was instead contacted with  $\varnothing$  200  $\mu$ m silver wires and silver paste (CN33-145Ag, Ferro, USA) to one of the multimeters.

In a third experiment, to compare the sensor to an ordinary calorimetric flow sensor with platinum sensor elements, the setup was altered, so that one multimeter measured the resistance through the zirconia upstream the heaters and the other measured the resistance through the upstream platinum element, where the latter employed 4-point probing. After sweeping the flow as above, the point of measurement was moved downstream the heaters, and the measurement was repeated. Moreover, to study the intrinsic noise of the two measurement principles, an AC coupled oscilloscope (DSO7104A, Agilent Tech., USA) was connected across the zirconia and platinum resistors at constant flows of 0.7 and 34 sccm, measuring the voltage noise between 0.5 and 250 Hz.

In Figure 2, the upstream and downstream resistances versus flow from the first set of experiments are shown. The change in resistance followed a similar behavior regardless of applied power, although the relative change increased with the resistance at zero flow. Starting from zero flow, the upstream resistance continuously increased, whereas the downstream resistance initially decreased, up to a flow of about 15 sccm, after which it also started increasing. The reason for this behavior is discussed in more detail below. The resistance at zero flow of the two resistors was initially more or less equal, but when returning to zero after sweeping the flow, they differed by up to 6%. However, after stabilizing for about 60 s after the measurement, they returned to their initial values. The reproducibility of the results was good, with the three 20-M $\Omega$  experiments differing by  $\sim$ 1.15%  $\pm$  0.09% ( $1\sigma$ ).

In a second experiment, where the sensor was placed in a furnace, it was found that the resistance between the two platinum conductors decreased exponentially with increased temperature.

Using two separate heaters to balance the resistances at zero flow, turned out to be useful. The total applied power showed the exponential dependence on the resistance at zero

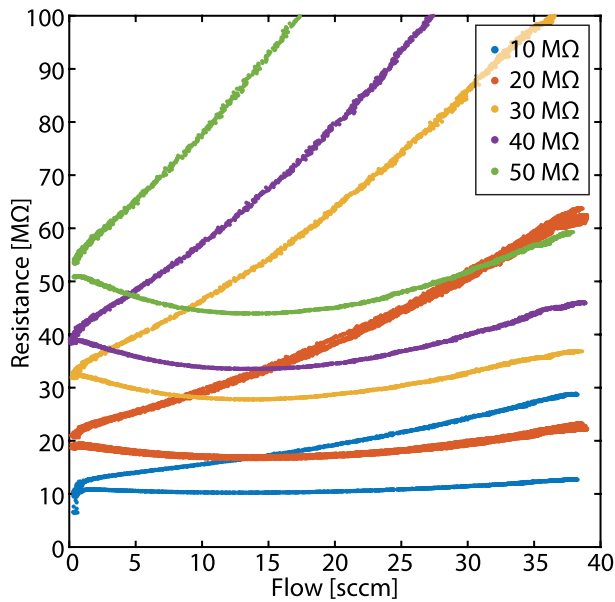


FIG. 2. Resistance change upstream and downstream of the heaters versus flow for five resistances at zero-flow. The resistances upstream the heaters increase monotonically, whereas those downstream initially decrease.

flow expected since the resistance in the zirconia was exponentially dependent on the temperature,<sup>15</sup> and the heater temperature was proportional to the supplied power.<sup>1,17</sup> Due to variations in the heater resistances stemming from fabrication,<sup>15</sup> the individual powers differed slightly. Still, the method enabled rapid initialization of the sensor with a precision of about 1% of the resistance at zero flow, which probably could be improved further by employing computer control with feedback.<sup>21</sup>

Defining the sensor output as the difference between the upstream and downstream resistors, the transfer curve of the sensor was more or less linear, Figure 3.

The corresponding sensitivities were obtained by linear fitting to this data, Figure 4. The sensitivity was found to improve linearly with the resistance at zero flow, reaching a maximum of 3.1 MΩ/sccm at 50 MΩ. With regard to noise, the sensor was found to pick up considerable interference at

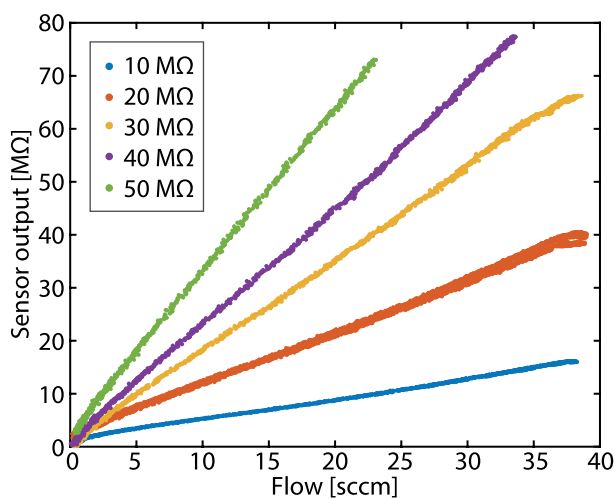


FIG. 3. Sensor output, i.e., the difference between the upstream and downstream resistances, versus flow.

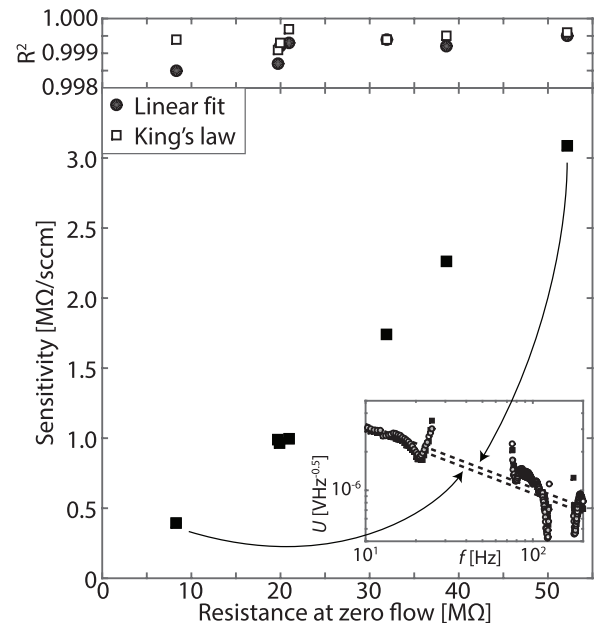


FIG. 4. Sensitivity of the sensor versus the resistance at zero flow (bottom), as calculated from linear fits to the sensor response (Figure 3). The goodness of these fits (black circles) was consistently higher than 0.998, and the goodness of the fits to King's law (white squares), which are described in detail, was even higher. The inset shows the voltage noise at the highest and the lowest temperature. Each spectrum was calculated from 2048 averages of 2 s long time series.

50 Hz, most likely from the common ground with the power supply. However, disregarding this outside noise source and its harmonics, the inherent noise of the sensor was found to be dominated by  $1/f$ -like noise at frequencies below 200 Hz. The amplitude of this noise increased only slightly with the resistance at zero flow, inset of Figure 4.

These results deviated from what is commonly observed in traditional calorimetric flow sensors, where linearity only is achieved over small flow intervals.<sup>1,15,19</sup> This was evident from the results of the experiment where the resistances through the outer platinum conductors were measured in parallel with the resistances through the zirconia, Figure 5. One major difference was the magnitude of the change in resistance, which was in the order of milliohms for the platinum elements and megaohms for the zirconia. More pronounced, however, was the difference in transfer curves, where the platinum sensor elements produced the expected response,<sup>1,15,16,19</sup> whereas the zirconia elements still exhibited a linear response.

This is due to the different measurement principles, where the resistance of the platinum and zirconia elements depended linearly and exponentially, respectively, on the temperature change induced by the flow. The relationship between the flow,  $F$ , and the induced temperature difference,  $\Delta T$ , in a flow sensor is commonly described by King's law,  $\Delta T = (\alpha + \beta F^n)^{-1}$ , where  $\alpha$  and  $\beta$  are constants, and  $n = 0.5$  in the ideal case.<sup>16</sup> This gives the transfer curve of the conventional sensor its characteristic appearance, since  $\Delta R \sim \Delta T$ . The zirconia sensor, consequently, should yield  $\Delta R \sim \exp(\Delta T) \sim \exp[(\alpha + \beta F^n)^{-1}]$ . In order to evaluate this assumption, equations on the form  $\Delta R(F) = a \exp[b(1 + cF^d)^{-1}]$ , where  $a$ ,  $b$ ,  $c$ , and  $d$  are constants, were fitted to the results in Figure 4.

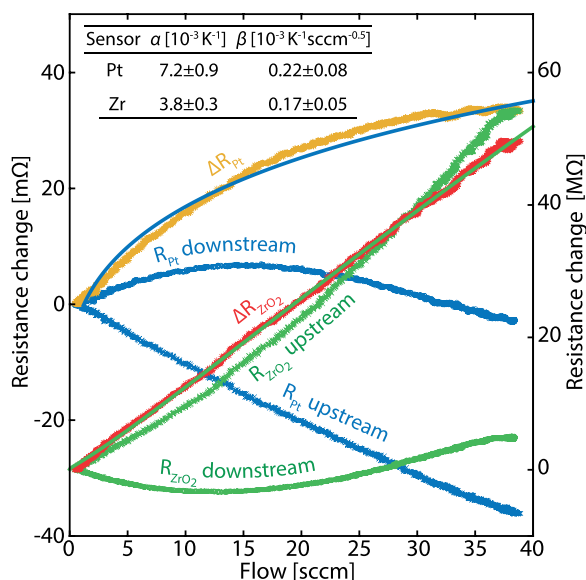


FIG. 5. Comparison between a calorimetric flow sensor with platinum (blue and left y axis) and zirconia (green and right y axis) sensing elements, showing the change in resistance of the upstream and downstream elements separately. The differences between the resistances, i.e., the sensor responses, are shown in yellow for platinum and maroon for zirconia, together with fits with King's law. The fitting parameters are shown in the inset with errors corresponding to  $3\sigma$ .

An example can be seen in Figure 5. The resulting  $R^2$ s were consistently better than the linear fits, Figure 4. Moreover, both fits in Figure 5 yielded  $\alpha$  and  $\beta$  in the same range (see inset of Figure 5). This attests that the zirconia sensor can be described by King's law, and that the exponential temperature dependence of its resistance is the main explanation for its excellent linearity in the studied flow range.

It should be remarked that the almost nine orders of magnitude higher sensitivity of the zirconia sensor does not necessarily make it superior, since resistance can be straightforwardly measured in both the milli- and megaohm range, although the former often require 4-point probing. Alternatively, the sensitivity can be expressed as the relative change in resistance per sccm, which for the experiment shown in Figure 5 was 0.24%/sccm and 5.1%/sccm for the platinum and zirconia sensors, respectively. Regarding accuracy and precision, the relative root-mean-square noise of the platinum sensor was about 20 times lower than that of the zirconia sensor, meaning that their signal-to-noise ratios were comparable. However, regarding linearity, the zirconia sensor was superior.

However, in preliminary experiments, it was also observed that the zirconia sensor elements were susceptible to interference from temperature changes in the bulk of the device. If subjected to high flow rates ( $>10$  sccm) over long times ( $>120$  s), also the bulk was cooled. This caused the resistance to change in a less predictable manner, and the signal to depend on, e.g., the thermal connection to the gas connectors and the PCB carrier. Moreover, this caused the sensor response to deviate strongly from the linear trends. To avoid this, quick measurements were conducted at low flow rates. If the sensor is to be used for higher flow rates or longer measurements, the zirconia resistors have to be isolated from

the thermal bulk of the device, e.g., by isolating them in thin membranes. Another potential problem with the sensor is ion depletion, although no signs of this have been observed, despite several hours of continuous operation, inset of Figure 4. This phenomenon should be investigated in more detail, and should it become a problem, it might be mitigated by an AC bias current. Other potential improvements include powering the heaters to a constant temperature at all flows.<sup>22</sup>

Disregarding the effect of temperature changes in the bulk, and with reference to Figure 6, the response of the sensor is interpreted as: (a) at low flow rates, the temperature profile in the gas is symmetric and centered over the heaters. As the flow increases, the profile is skewed and shifted downstream, creating a temperature difference in the zirconia upstream and downstream of the heaters. (b) At a slightly higher flow rate, here around 15 sccm, the temperature profile is centered on the active part of the zirconia downstream of the heaters. (c) As the flow continues to increase, the temperature profile is shifted further down the channel, and the temperature in both elements starts to decrease monotonically. The sensor signal is expected to cease when the flow rate becomes so high that the heaters cannot maintain their temperature. At this point, the heat transfer between the heaters and sensing elements will be limited and occur mainly by conduction in the substrate.

In this paper, a calorimetric flow sensor based on the temperature dependent resistivity of ion conducting zirconia has been presented. This sensor was shown to exhibit a sensitivity of up to 3.1 M $\Omega$ /sccm, or 6.0%/sccm, and to be linear over a wide flow range of about 0–40 sccm, with an  $R^2$  in the order of 0.999. The fact that the sensors endured high temperatures, makes it very promising for a wide range of applications, e.g., for integration inside the thruster nozzle of a spacecraft propulsion system.

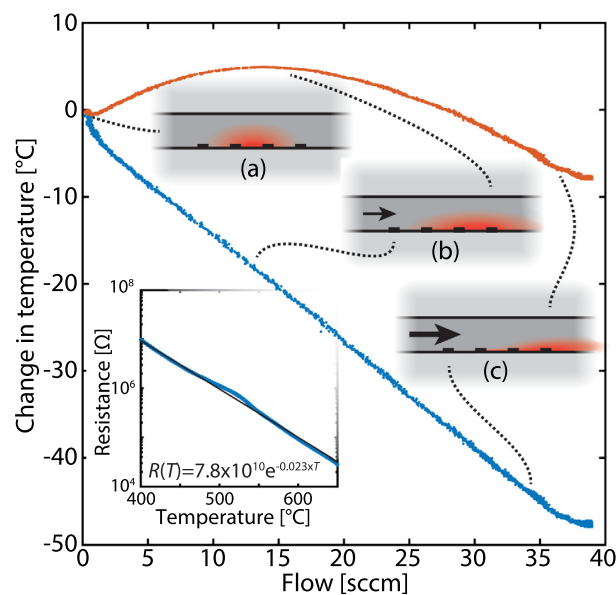


FIG. 6. Approximated change in temperature upstream (blue) and downstream (red) of the heaters versus flow for a resistance at zero flow of 20 M $\Omega$ . The inset shows the relationship between resistance and temperature from a calibration measurement in a furnace together with a fitted exponential curve. The heat profile in the gas at different flows is illustrated by (a)–(c).

Dr. Kristoffer Palmer at NanoSpace AB is gratefully acknowledged for helpful discussions. The Swedish Governmental Agency of Innovation Systems (VINNOVA) and the Swedish National Space Board are acknowledged for funding this project. The Knut and Alice Wallenberg Foundation was acknowledged for laboratory funding.

- <sup>1</sup>V. Lekholm, A. Persson, K. Palmer, F. Ericson, and G. Thornell, *J. Micromech. Microeng.* **23**, 055004 (2013).
- <sup>2</sup>K. H. Cheah, P. S. Khiew, and J. K. Chin, *J. Micromech. Microeng.* **22**, 095013 (2012).
- <sup>3</sup>J. Xiong, S. Zheng, Y. Hong, J. Li, Y. Wang, W. Wang, and Q. Tan, *J. Zhejiang Univ., Sci., C* **14**(4), 258 (2013).
- <sup>4</sup>T.-A. Grönland, P. Rangsten, M. Nese, and M. Lang, *Acta Astronaut.* **61**, 228 (2007).
- <sup>5</sup>J. Köhler, J. Beijhed, H. Kratz, U. Lindberg, K. Hjort, and L. Stenmark, *Sens. Actuat. A* **97–98**, 587 (2002).
- <sup>6</sup>K. W. Schlichting, N. P. Padture, and P. G. Klemens, *J. Mater. Sci.* **36**, 3003 (2001).
- <sup>7</sup>J. F. Shackelford and R. H. Doremus, *Ceramic and Glass Materials* (Springer-Verlag, New York, 2008), pp. 169–197.
- <sup>8</sup>A. G. Belous, O. I. V'yunov, V. Gunes, and O. Bohnke, *Inorg. Mater.* **50**(12), 1235 (2014).
- <sup>9</sup>M. Filal, C. Petot, M. Mokchah, C. Chateau, and J. L. Carpentier, *Solid State Ionics* **80**, 27 (1995).
- <sup>10</sup>R. M. Ormerod, *Chem. Soc. Rev.* **32**, 17 (2003).
- <sup>11</sup>E. V. Tsipis and V. V. Kharton, *J. Solid State Electrochem.* **12**, 1367 (2008).
- <sup>12</sup>J.-H. Lee, *J. Mater. Sci.* **38**, 4247 (2003).
- <sup>13</sup>N. Miura, T. Sato, S. A. Anggrain, H. Ikeda, and S. Zhuiykov, *Ionics* **20**, 901 (2014).
- <sup>14</sup>W. C. Maskell, *Solid State Ionics* **134**, 43 (2000).
- <sup>15</sup>V. Lekholm, A. Persson, L. Klintberg, and G. Thornell, "Investigation of a zirconia co-fired ceramic calorimetric microsensor for high-temperature flow measurements," *J. Micromech. Microeng.* (submitted).
- <sup>16</sup>M. Elwenspoek, in *Proceedings of the 1999 International Conference on Semiconductor, Vol. 2* (IEEE, 1999), p. 423.
- <sup>17</sup>J. T. W. Kuo, L. Yu, and E. Meng, *Micromachines* **3**, 550 (2012).
- <sup>18</sup>N. T. Nguyen, "Micromachined flow sensors—A review," *Flow Meas. Instrum.* **8**(1), 7–16 (1997).
- <sup>19</sup>K. Palmer, H. Kratz, H. Nguyen, and G. Thornell, *J. Micromech. Microeng.* **22**, 065015 (2012).
- <sup>20</sup>U. Schmid, *Sens. Actuat. A* **97–98**, 253 (2002).
- <sup>21</sup>P. Bruschi, M. Dei, and M. Piotta, *IEEE Sens. J.* **11**, 1162 (2011).
- <sup>22</sup>B. W. van Oudheusden, *Sens. Actuat. A* **30**, 5–26 (1992).